

Journal of Applied Phycology

Effect of glycerol and Ca²⁺ addition on physicochemical properties of edible carrageenan/porphyran based films obtained from *Pyropia columbina* red seaweed. --Manuscript Draft--

Manuscript Number:	JAPH-D-14-00427R1
Full Title:	Effect of glycerol and Ca ²⁺ addition on physicochemical properties of edible carrageenan/porphyran based films obtained from <i>Pyropia columbina</i> red seaweed.
Article Type:	Original Research
Keywords:	Edible films; red seaweeds; phycocolloids; calcium; plasticizers.
Corresponding Author:	Pablo Rodrigo Salgado, Ph.D. CIDCA (CONICET-UNLP) La Plata, Buenos Aires ARGENTINA
Corresponding Author Secondary Information:	
Corresponding Author's Institution:	CIDCA (CONICET-UNLP)
Corresponding Author's Secondary Institution:	
First Author:	Raúl E Cian, Ph.D.
First Author Secondary Information:	
Order of Authors:	Raúl E Cian, Ph.D. Pablo Rodrigo Salgado, Ph.D. Silvina R Drago, Ph.D. Adriana N Mauri, Ph.D.
Order of Authors Secondary Information:	
Abstract:	<p>The aim of this work was to study the effect of glycerol and Ca²⁺ addition on physicochemical properties of phycocolloids (carrageenans/porphyrans) based films obtained from <i>Pyropia columbina</i> aqueous fraction. Films were formed by casting from aqueous dispersions of phycocolloids-enriched fraction (P) with different levels of glycerol (0, 12.5 and 25 g/100 g dry solid) and the optional addition of Ca²⁺ (16 g/100 g dry solid), yielding 6 formulations according to a multi-factorial design (P, PG1, PG2, PCa, PCaG1 and PCaG2). All films were homogeneous, flexible and slightly greenish. Moisture content, water solubility and water vapor permeability of films were significantly increased by adding glycerol to the formulation (11%, 12% and 6%, respectively). Increasing glycerol content in formulations (12.5 to 25 g/100 g dry solid), allow obtaining more stretchable but less resistant films (with less tensile strength and elastic modulus) than those produced without plasticizer (P). Ca²⁺ addition masked glycerol effect in some properties (water solubility and water vapor permeability), but in others, the effect of Ca²⁺ was added to the plasticizer glycerol effect (mechanical properties). Ca²⁺ could stabilize the three-dimensional structure of P phycocolloids by interactions between sulfate groups, promote water retention and open film structure. Use of these additives yielded films from <i>Pyropia columbina</i> with a wide range of mechanical properties, thus extending the scope of these materials.</p>
Response to Reviewers:	The manuscript was modified according to the suggestions of reviewers. All modifications are highlighted in red in the revised manuscript.

1 **Effect of glycerol and Ca⁺² addition on physicochemical properties of edible**
2 **carrageenan/porphyran based films obtained from *Pyropia columbina* red seaweed**

3
4 Raúl E. Cian^{1,2}, Pablo R. Salgado^{*2,3}, Silvina R. Drago^{1,2} and Adriana N. Mauri^{2,3}

5
6 ¹Instituto de Tecnología de Alimentos, Facultad de Ingeniería Química, Universidad

7 Nacional del Litoral, 1° de Mayo 3250, (3000) Santa Fe, República Argentina.

8 ²Consejo Nacional de Investigaciones Científicas y Técnicas (CONICET), Av.

9 Rivadavia 1917, (C1033AAJ) Ciudad de Buenos Aires, República Argentina.

10 ³Centro de Investigación y Desarrollo en Criotecnología de Alimentos (CIDCA),
11 CONICET CCT La Plata y Facultad de Ciencias Exactas, Universidad Nacional de La

12 Plata, 47 y 116 S/N°, (B1900JJ) La Plata, República Argentina.

13
14 *Author to whom correspondence should be addressed: Telephone/Fax: 54 -221-

15 4890741. E-mail: psalgado78@gmail.com

16

17 **Abstract**

18 The aim of this work was to study the effect of glycerol and Ca^{+2} addition on
19 physicochemical properties of phycocolloids (carrageenans/porphyrans) based films
20 obtained from *Pyropia columbina* aqueous fraction. Films were formed by casting from
21 aqueous dispersions of phycocolloids-enriched fraction (P) with different levels of
22 glycerol (0, 12.5 and 25 g/100 g dry solid) and the optional addition of Ca^{+2} (16 g/100 g
23 dry solid), yielding 6 formulations according to a multi-factorial design (P, PG₁, PG₂,
24 PCa, PCaG₁ and PCaG₂). All films were homogeneous, flexible and slightly greenish.
25 Moisture content, water solubility and water vapor permeability of films were
26 significantly increased by adding glycerol to the formulation (11%, 12% and 6%,
27 respectively). Increasing glycerol content in formulations (12.5 to 25 g/100 g dry solid),
28 allow obtaining more stretchable but less resistant films (with less tensile strength and
29 elastic modulus) than those produced without plasticizer (P). Ca^{+2} addition masked
30 glycerol effect in some properties (water solubility and water vapor permeability), but in
31 others, the effect of Ca^{+2} was added to the plasticizer glycerol effect (mechanical
32 properties). Ca^{+2} could stabilize the three-dimensional structure of **P** phycocolloids by
33 interactions between sulfate groups, promote water retention and open film structure.
34 Use of these additives yielded films from *Pyropia columbina* with a wide range of
35 mechanical properties, thus extending the scope of these materials.

36

37 *Keywords:* Edible films, red seaweeds, phycocolloids, calcium, plasticizers.

38

39 **Introduction**

40 Over the last years, marine microorganisms such as bacteria, microalgae and seaweeds
41 have represented a large source of valuable materials (Leiria Campo et al. 2009). In this
42 way, the three commercially exploited carbohydrate polymers (phycocolloids) from
43 these marine microorganisms are: (1) alginates from brown seaweeds, (2) carrageenans,
44 and (3) agar both isolated from red seaweeds (Souza et al. 2012).

45 Carrageenans are water-soluble polymers with a linear chain of partially sulfated
46 galactans, which have high potentiality as film-forming material. The number and
47 position of sulfate groups on the disaccharide repeating unit determine the classification
48 in three major types: lamda (λ), kappa (κ), and iota (ι) (Al-Alawi et al. 2011), which
49 have sulfate contents of 41%, 33% and 20% (w/w), respectively, resulting from one,
50 two and three sulfate ester groups per dimeric unit (Karbowski et al. 2006). The main
51 difference between the highly sulphated carrageenans from the less sulphated agars is
52 the presence of D-galactose and anhydro-D-galactose in carrageenans and D-galactose,
53 L-galactose or anhydro-L-galactose in agars (Gómez-Ordóñez and Rupérez 2011).
54 Noteworthy that porphyrans are the main agar from *Pyropia* genus. These sulfated
55 polysaccharides comprising the hot-water soluble portion of the cell wall and
56 intercellular region (Zhang et al. 2005).

57 These phycocolloids have been used for the development of biodegradable films with
58 good mechanical and barrier properties (Blanco Pascual et al. 2014; Giménez et al.
59 2013; Karbowski et al. 2006; Rhim 2012; Sousa et al. 2010). In this sense, these films
60 can inhibit/regulate the migration of moisture, oxygen, carbon dioxide, lipids, and also
61 carry food ingredients to improve food properties **when they are used as** packaging
62 (Martins et al. 2012).

63 In a previous work, edible films were prepared from aqueous fractions extracted from
64 *Pyropia columbina* red seaweed (found on hard substratum in Patagonia Argentina
65 coasts) without ulterior purification steps, which implies a lower cost process than the
66 use of purified phycocolloids fractions (carrageenans and agars). These films –
67 processed without the addition of any plasticizer– showed high tensile strength, low
68 elongation at break and interesting antioxidant properties (Cian et al. 2014).

69 It is known that physicochemical properties of biopolymers films could be modified by
70 the addition of plasticizers or cross-linking agents (Han and Gennadios, 2005; Baldwin
71 et al. 2012). Glycerol, a low molecular weight and non-volatile polyol, is widely used as
72 plasticizer and its addition to these polysaccharides films could significantly improve
73 their flexibility and guarantee their processability (Vieira et al. 2011). Calcium, being a
74 divalent cation, is capable of forming intra-molecular bridges between the sulphate
75 groups of adjacent anhydro-d-galactose and d-galactose residues, and it was reported
76 that its presence favoured carrageenan gelation (Thrimawithana et al. 2010). The effect
77 of calcium on alginate edible films has been studied (Olivas and Barbosa-Cánovas
78 2008; Sartori et al. 1997; Rhim, 2004), but it is not the case for carrageenans/porphyrans
79 films from *P. columbina*. As far as we know, there are no published works related to the
80 production of carrageenans/porphyrans based films with plasticizers from this seaweed
81 and even less with addition of calcium.

82 The aim of this work was to study the effect of glycerol and Ca^{+2} additions on
83 physicochemical properties of phycocolloids (carrageenans/porphyrans) based films
84 obtained from *Pyropia columbina* aqueous fraction.

85

86 **Materials and Methods**

87 ***Preparation of phycocolloids (carrageenans/porphyrans) fraction from P.***
88 ***columbina***

89 One kilogram of different specimens of *P. columbina* was hand-picked in Punta
90 Maqueda (46°00'S, 67°34'W) in spring time. Punta Maqueda, a pristine beach far away
91 from anthropogenic activities, is located within San Jorge Gulf at 30 km to the south of
92 Comodoro Rivadavia, Argentina. Samples were taken to the laboratory at 4°C inside
93 plastic bags. To remove adherent seawater, sediment, organic debris, macro fauna and
94 epibiota, they were scraped and rinsed with distilled water. *P. columbina* samples were
95 dried to environment temperature (22 - 25°C), ground to obtain a powder with a particle
96 size lower than 1 mm, using a laboratory hammer mill (Retsch, Haan, Germany). Then,
97 samples were passed through a 20-mesh sieve (0.85 mm) and stored at 4°C in plastic
98 bags until analysis.

99 Phycocolloids-enriched fraction (**P**) from *P. columbina* was prepared as follow. *P.*
100 *columbina* algae powder was dispersed at 50 **g/kg** in cold distilled water (at 4°C) for 2 h
101 and filtered through a 50-mesh sieve (0.297 mm). The residue of the filtration (particle
102 size > 0.297 mm) was subjected to two washings with cold distilled water (4°C), was
103 dispersed at 50 **g/kg** in hot distilled water (at 95°C) for 2 h and then, centrifuged at
104 3000xg for 45 minutes at 45°C. The supernatant obtained from hot distilled water
105 extraction was Phycocolloids-enriched fraction and had **1 g/100 g dry solid**. **P**
106 composition in dry base was: protein: 14.3%, total carbohydrates: 72%, sulphate
107 content: 12.6% and ash: 6.4%. The chlorophyll *a* and total chlorophyll content from **P**
108 was determinate spectrophotometrically according to Wolfenden et al. (1988).

109 ***Films preparation***

110 Films were prepared by casting from aqueous dispersions of phycocolloids-enriched
111 fraction (**P**) (1 g dry solid/100 g dispersion) with different amounts of glycerol (0, 12.5
112 and 25 g/100 g dry solid) and the optional addition of Ca^{+2} (16 g/100 g dry solid),
113 yielding 6 formulations according to a multi-factorial design. Formulations were named
114 as follow: **P**, **PG₁** (**P** + 12.5 g glycerol/100 g dry solid), **PG₂** (**P** + 25 g glycerol/100 g
115 dry solid), **PCa** (**P** + 16 g Ca^{+2} /100 g dry solid), **PCaG₁** (**P** + 12.5 g glycerol/100 g dry
116 solid + 16 g Ca^{+2} /100 g dry solid) and **PCaG₂** (**P** + 25 g glycerol/100 g dry solid + 16 g
117 Ca^{+2} /100 g dry solid).

118 The film-forming dispersions were agitated in a magnetic stirrer for 1 hour at room
119 temperature. Twenty mL of each film-forming dispersion were poured on polystyrene
120 Petri dishes (64 cm²) and then dehydrated at 60°C for 5 h in an oven with air flow
121 circulation (Yamato, DKN600, USA). Resulting films were conditioned 48 h at 20°C
122 and 58% relative humidity (RH) in desiccators with saturated solutions of NaBr before
123 being peeled from the casting surface for characterization.

124 *Rheology of film-forming dispersions*

125 Rotational analyses of **P**, **PG₁**, **PG₂**, **PCa**, **PCaG₁** and **PCaG₂** film-forming dispersions
126 were performed at 25 °C in a Haake ReoStress 600 (Thermo Haake, Karlsruhe,
127 Germany) with a 1 mm gap serrated plate–plate sensor system PP35. Dispersions were
128 maintained at 25°C by a circulating water bath (Circulator DC50 Thermo Haake,
129 Germany) connected to the jacket surrounding the sensor system during testing. Shear
130 stress (τ) was determined as a function of shear rate (D). The shear rate was increased
131 from 0 to 500 s⁻¹ in 2 min, was maintained for 1 min and then, decreased from 500 to 0
132 s⁻¹ in 2 min. Flow (n) and consistency (K) indexes were determined adjusting
133 experimental results with the Ostwald de Waele model (equation 1).

134
$$\tau = K .D^n \quad (1)$$

135 Where: τ is the shear stress (Pa), K is the consistency index (Pa sⁿ), D is the shear rate
136 (s⁻¹) and n is the flow index (dimensionless).

137 Apparent viscosities (η_{app} , mPa s) were calculated in the upwards curves at 60, 300 and
138 500 s⁻¹ for each film-forming dispersion.

139 Determinations were carried out in triplicate.

140 ***Film characterization***

141 *Thickness*

142 Film thickness was measured by a digital coating thickness gauge (Check Line DCN-
143 900, USA). Measurements were done at five positions along the rectangular strips for
144 the tensile test, and at the center and at eight positions round the perimeter for the water
145 vapor permeability (WVP) determinations. The mechanical properties and WVP were
146 calculated using the average thickness for each film replicate.

147 *Color*

148 Film color was determined with a Konica Minolta Chroma Meter CR-400 (Konica
149 Minolta Chroma Co., Osaka, Japan) set to C illuminant/2° observer. A CIE-Lab color
150 scale was used to measure the degree of lightness (L^*), redness ($+a^*$) or greenness ($-$
151 a^*), and yellowness ($+b^*$) or blueness ($-b^*$) of the films. The instrument was calibrated
152 using a white standard plate with color coordinates of $L^*_{standard} = 97.55$, $a^*_{standard} = -$
153 0.03 and $b^*_{standard} = 1.73$ provided by Minolta. Films color was measured on the surface
154 of this standard plate and total color difference (ΔE^*) was calculated as follow:

155
$$\Delta E^* = [(L^*_{film} - L^*_{standard})^2 + (a^*_{film} - a^*_{standard})^2 + (b^*_{film} - b^*_{standard})^2]^{0.5} \quad (2)$$

156 Color can also expressed by use of polar (or cylindrical) coordinates L^* , C^* and h^* ,
157 where L^* is the same as previously, C^* is chroma or saturation index and H^* is hue.
158 The following equations were used to convert $L^*a^*b^*$ coordinates to $L^*C^*h^*$
159 coordinates.

$$160 \quad C^* = (a^{*2} + b^{*2})^{0.5} \quad (3)$$

$$161 \quad h^* = \arctan (b^*/a^*) \quad (4)$$

162 Values were expressed as the means of nine measurements on different areas of each
163 film.

164 *Opacity*

165 Each film specimen was cut into a rectangular piece and placed directly in a
166 spectrophotometer test cell, and measurements were performed using air as the
167 reference. A spectrum of each film was obtained in an UV-Vis spectrophotometer
168 (Beckman DU650, Germany). The area under the absorption curve from 400 to 800 nm
169 was recorded (AU x nm) and divided by film thickness (nm) (García et al. 2006). The
170 opacity of films was expressed as absorbance units (AU). **Five replications for each**
171 **formulation were performed.**

172 *Moisture content (MC)*

173 Small specimens of films collected after conditioning were cut and placed on Petri
174 dishes that were weighed before and after oven drying at 105°C for 24 h (ASTM D644-
175 99, 2004). MC values were determined in triplicate for each film, and calculated as the
176 percentage of weight loss relative to the initial weight.

177 *Water solubility (WS)*

178 WS was determined following the method described by Gontard et al. (1994) with slight
179 modifications. Film portions were weighed (diameter = 2 cm; $P_o \sim 0.03-0.05\text{g}$) and
180 placed in an Erlenmeyer flask (250 mL) with 50 mL of distilled water (containing
181 0.02% w/v sodium azide) and then sealed and shaken at 100 rpm for 24 h at 20°C
182 (Ferca, TT400 model, Argentina). The solution was then filtered through Whatman n°1
183 filter paper (previously dried and weighed) to recover the remaining undissolved film,
184 which was desiccated at 105°C for 24 h (P_f). WS was calculated as follows:

185

$$WS = [(P_o \cdot (100 - MC)) - P_f] \cdot 100 / [P_o \cdot (100 - MC)] \quad (5)$$

186 Where P_o = initial film weight (g), P_f = final dry film weight (g), MC = moisture content
187 (%). **WVP tests were carried out in triplicate.**

188 *Water vapor permeability (WVP)*

189 Water vapor permeability tests were conducted according to ASTM method E96-00
190 (ASTM, 2004) with some modifications. Each film sample was sealed over a circular
191 opening of 0.00185 m² in a permeation cell that was stored at 20°C in desiccators. To
192 maintain a 75% relative humidity (RH) gradient across the film, anhydrous silica (0%
193 RH_c) was placed inside the cell and a saturated NaCl solution (75% RH_d) was used in
194 the desiccators. The RH inside the cell was always lower than outside, and water vapor
195 transport was determined from the weight gain of the permeation cell. When steady-
196 state conditions were reached (about 1 h), eight weight measurements were made over 5
197 h. Changes in the weight of the cell were recorded and plotted as a function of time. The
198 slope of each curve ($\Delta m/\Delta t$, g H₂O s⁻¹) was obtained by linear regression and the water
199 vapor transmission rate was calculated from the slope divided by the permeation cell
200 area (A, m²). WVP (g H₂O Pa⁻¹ s⁻¹ m⁻¹) was calculated as:

201
$$\text{WVP} = [\text{WVTR} / (P_{\text{V}}^{\text{H}_2\text{O}} \cdot (\text{RH}_d - \text{RH}_c))] \cdot d \quad (6)$$

202 Where; WVTR: water vapor transmission rate ($\text{g H}_2\text{O s}^{-1} \text{ m}^{-2}$); $P_{\text{V}}^{\text{H}_2\text{O}}$: saturation water
203 vapor pressure at test temperature (2339.27 Pa at 20 °C); ($\text{RH}_d - \text{RH}_c$): relative humidity
204 gradient across the film, expressed as a fraction (0.75); A: permeation (m^2) area; and d:
205 film thickness (m). Each WVP value represents the mean value of at least three samples
206 taken from different films.

207 *Mechanical properties*

208 Tensile strength (TS), elastic modulus (EM) and elongation at break (EAB) of the films
209 were determined using a texture analyzer TA.XT2i (Stable Micro Systems, Surrey,
210 England) equipped with a tension grip system A/TG, according the procedures outlined
211 in the ASTM method D882-02 (ASTM, 2004). The measurements were made at 20°C
212 and 65% RH in a controlled room. Films probes of 70 mm length and 6 mm width were
213 used, a minimum of six probes were prepared from each film. The initial grip separation
214 was set at 50 mm and the crosshead speed at 0.5 mm s^{-1} . The curves of force (N) as a
215 function of distance (mm) were recorded by the Texture Expert V.1.15 software (Stable
216 Micro Systems, Surrey, England). Tensile properties were calculated from the plot of
217 stress (tensile force/initial cross-sectional area) versus strain (extension as a percentile
218 of the original length). TS and EAB were determined directly from the stresses-strain
219 curves, and EM was determined as the slope of the initial linear portion of this curve.
220 Twelve replications for each formulation were performed.

221 *Scanning electron microscopy (SEM) of films*

222 SEM of films cross-section (cryofractured by immersion in liquid nitrogen) and films
223 surface were performed. The pieces of films were mounted on aluminum stubs using a
224 double-sided tape and were coated with a thin gold layer using a cool sputter system

225 (SCD 005, BAL–TEC, Switzerland). SEM images were acquired with a scanning
226 electron microscope (XL-20, Philips, Netherlands), using an acceleration voltage of 20
227 kV for all the samples.

228 *FTIR analysis*

229 Infrared spectra of studied films was acquired using a Nicolet iS 10 Infrared
230 Spectrometer (Thermo Scientific, Madison, WI, USA). Measurements were performed
231 at room temperature. Spectra were obtained in the 4000-400 cm^{-1} range by
232 accumulation of 60 scans at 4 cm^{-1} resolution. FTIR spectra were recorded using the
233 OMNIC software version 7.3 (Thermo Electron Corporation, USA). Prior to sample
234 collection, a background spectrum was recorded and subtracted from sample spectra.
235 The spectra were baseline corrected at 1812 cm^{-1} and normalized for comparison
236 purposes. **Two replications for each formulation were performed.**

237 *Statistical analysis*

238 Results were expressed as mean \pm standard deviation and were analyzed by analysis of
239 variance (ANOVA). Means were tested with the Fisher's least significant difference test
240 for paired comparison, with a significance level $\alpha=0.05$, using the Statgraphics Plus
241 version 5.1 software (Statgraphics, USA).

242

243 **Results and Discussion**

244 *Rheology of film-forming dispersions*

245 Rheological behavior of film-forming dispersions obtained from phycocolloids-enriched
246 fractions (**P**) added with glycerol and/or calcium is shown in **Table 1**. All dispersions
247 exhibited a **non-Newtonian shear-thinning behavior ($n<1$)**. The power-law (or the

248 Ostwald de Waele model) fitted satisfactorily with the experimental data ($r^2 > 0.98$) for
249 **P**, **PG₁**, **PG₂**, **PCa**, **PCaG₁** and **PCaG₂** film-forming dispersions. The corresponding
250 fitting parameters, n and K are shown in **Table 1**. These results agree with Marcotte et
251 al. (2001) and Lizarraga et al. (2006) who worked with carrageenan aqueous
252 dispersions, at similar concentration and temperature. The incorporation of glycerol to
253 film-forming dispersions –with or without Ca^{2+} – did not modify its rheological
254 properties. **P**, **PG₁** and **PG₂** dispersions, which differed in its glycerol concentrations,
255 showed similar consistency and flow indexes (K and n) and similar apparent viscosities
256 (calculated at 60, 300 and 500 s^{-1}) ($p > 0.05$). The same effect was observed for **PCa**,
257 **PCaG₁** and **PCaG₂** dispersions ($p > 0.05$). The presence of Ca^{2+} in film-forming
258 dispersions produced an important decrease in K and a slightly increase in n ($p < 0.05$),
259 that only was reflected in the apparent viscosities at low deformations, as **P**, **PG₁** and
260 **PG₂** film-forming dispersions have higher values of apparent viscosity than **PCa**,
261 **PCaG₁** and **PCaG₂** ($p < 0.05$) (only at 60 s^{-1}) (**Table 1**). This suggests that the addition
262 of calcium hindered the polymer–polymer interactions in **P**, **PG₁** and **PG₂** dispersions.
263 Plasticizer and cross-linking effects expected by adding glycerol and Ca^{2+} were not
264 reflected in the rheology of the film forming dispersions.

265

266 *Film characterization*

267 *Appearance and microstructure*

268 All phycocolloids-based films, with or without glycerol and Ca^{2+} , were found to be
269 homogeneous and flexible. **Table 2** shows their thickness, color parameters and opacity.
270 **P**, **PG₁** and **PG₂** films had similar thickness values ($\sim 17 \mu\text{m}$) ($p > 0.05$), indicating that
271 glycerol addition not affect this property. In contrast, addition of Ca^{2+} significantly

272 increased film thickness (~21 μm) ($p < 0.05$). This result agrees with Rhim (2004), who
273 worked with alginate films with different levels of calcium chloride (0.01, 0.02, and
274 0.03 g CaCl_2/g alginate). In this work, the authors found that thickness of alginate films
275 made with 0.03 g CaCl_2/g alginate were significantly higher than those obtained for
276 alginate alone. This effect on film thickness could be attributed to the binding of Ca^{2+} to
277 phycocolloids matrix. Janaswamy and Chandrasekaran (2002) found that calcium ions
278 and κ -carrageenan forms a threefold, right-handed, half-staggered, parallel, double
279 helix of 26.42 \AA pitch, stabilized by hydrogen bonds. In this context, the strong
280 interactions between the sulfate groups of neighboring helices, mediated by calcium
281 ions and water molecules, could be responsible for stabilizing these three-dimensional
282 structures of higher thickness.

283 CIE-Lab color parameters (L^* , a^* and b^*), total color difference (ΔE^*), chroma (C^*),
284 hue (h) and opacity of films give an idea of the visual aspect of the developed
285 materials. All films present a greenish coloration, that was characterized by negative
286 a^* values, given mainly by chlorophyll pigments that are present in *P. columbina*. In
287 this regard, chlorophyll *a* and total chlorophyll content from **P** was 3.4 ± 0.2 and $3.6 \pm$
288 $0.1 \mu\text{g/g}$, respectively. Film's color was modified only by the addition of Ca^{2+} . **PCa**,
289 **PCaG₁** and **PCaG₂** films had lower L^* , a^* and b^* values than those obtained from **P**,
290 **PG₁** and **PG₂** films ($p < 0.05$). However, no significant differences were obtained for
291 ΔE^* , C^* and h values ($p > 0.05$) from different films. The reduction of L^* , a^* and b^*
292 also was observed by Rhim (2004) for alginate films with 0.12 g $\text{CaCl}_2/100$ g
293 polysaccharide.

294 Film opacity is a critical property if the film will be used as a surface food coating.
295 Transparent films are characterized by low values of the area below the absorption

296 curve. As shown in **Table 2**, glycerol addition decreased the opacity of the resulting
297 films ($p < 0.05$) while the presence of Ca^{2+} did not affect it ($p > 0.05$). In this sense,
298 **PG₁**, **PG₂**, **PCaG₁** and **PCaG₁** films were less opaque than **P** and **PCa** ones. These
299 results agree with those reported by García et al. (2006) for corn starch and chitosan
300 films plasticized by glycerol. It is noteworthy that, Ca^{2+} addition did no increase film
301 opacity as happens in other polysaccharides based films (Fang et al. 2002; Fabra et al.
302 2010).

303 Undoubtedly, intense color limits some potential applications of these materials in
304 food packaging. For example, they could not be used for products that should be
305 easily visible through the package (such as minimally processed vegetables) because
306 the impaired visualization may reduce the acceptability of potential consumers. In
307 contrast, such films could be used, if their properties are adequate, for applications in
308 where color is irrelevant or in those where color may have an additional usefulness, as
309 in the case of packaging products that are sensitive to visible light radiations (i.e. that
310 can be altered or degraded by 400-800 nm light radiations), such as dairy products,
311 baby foods, soy based sauces, nutritional or medicinal products (Salgado et al. 2010;
312 Krikor et al. 2011).

313 *Water susceptibility of films*

314 The main disadvantage of films derived from biopolymers is their high water
315 susceptibility, which in general is affected by the hydrophilic or hydrophobic nature
316 of the plasticizers and cross-linkers added to formulation to modify their mechanical
317 properties. **Table 3** shows moisture content (MC), water solubility (WS) and water
318 vapor permeability (WVP) of the obtained films. Glycerol addition significantly
319 increases the moisture content of films with or without Ca^{2+} (**PG₁**, **PG₂**, **PCaG₁** and

320 **PCaG₂**). This result was expected since glycerol is a highly hygroscopic molecule
321 generally added into film-forming dispersions to prevent film brittleness (Shaw et al.
322 2002). In this sense, Karbowski et al. (2006) found that water content of carrageenan
323 films was far more sensitive to relative humidity when glycerol was included. In that
324 work, the authors showed that glycerol increases the water sorption of carrageenan
325 film and this increment becomes more significant at water activity above 0.7, whereas
326 no significant difference is noticeable for water sorption at lower water activities. It is
327 noteworthy that the addition of Ca⁺² also increased the moisture content of films.
328 Therefore, Ca²⁺ addition not only could be stabilizing the three-dimensional structure
329 of **P** phycocolloids by interactions between sulfate groups but also promoting water
330 retention. This was corroborated, since moisture content of **PCa** was significantly
331 higher than that of **P** (p<0.05). **PCaG₁** and **PCaG₂** exhibited the highest moisture
332 content (~19%), indicating that Ca⁺² exerts an additional effect with glycerol. Films´
333 water solubility showed a similar behavior to moisture content. **P** films had the lowest
334 WS (~85%) (**Table 2**). This property significantly increased in **PG₁** and **PG₂** films
335 with glycerol addition (p<0.05) and in **PCa** with Ca⁺² addition (p<0.05), and was the
336 highest in **PCaG₁** and **PCaG₂** films (~98%). This effect is commonly found by
337 adding glycerol to formulations based on biopolymers and is favored precisely
338 because the hydrophilic nature of the molecule (Baldwin et al., 2012). In the case of
339 Ca⁺², it is clear that any additional interactions that could be formed among
340 phycocolloids chains bridged by these ions are unstable in water, this being facilitated
341 by the greater thickness of the respective films and its greater water content.

342 **Table 3** also shows WVP of the studied films. As can be seen the addition of glycerol
343 to **P** matrix increase WVP. This phenomenon is related to the ability of the plasticizer
344 to establish favourable hydrogen bonds with the polymer, thereby disrupting

345 intermolecular polymer interactions (this mechanism being favoured by high relative
346 humidities), with consequent increase of polymer chain mobility and decreasing film
347 barrier properties (Gontard et al. 1993; Hernández-Muñoz et al. 2004). Similar value
348 of WVP was reported by Martins et al. (2012) for κ -carrageenan film with 30 g
349 glycerol/100 g polysaccharide. On the other hand, the addition of Ca^{2+} increase the
350 WVP, regardless of the glycerol presence, suggesting that high Ca^{2+} level mask the
351 glycerol effect. Additionally, **PCa**, **PCaG₁** and **PCaG₂** films exhibit the greater
352 thickness. As reported previously for other hydrophilic films (pectin, amylose,
353 cellulose ethers, sodium caseinate, and soybean proteins), WVP increases with film
354 thickness (Ghorpade et al. 1995).

355 *Mechanical properties of films*

356 Tensile strength (TS), elongation at break (EAB) and elastic modulus (EM) of the
357 films are shown in **Figure 1.A, B** and **C**, respectively. Mechanical properties of **P**
358 films were very interesting. Even without the requirement of a plasticizer, films were
359 flexible and had very high TS (~50 MPa) and EM (~29.5 MPa), but had low EAB
360 (~3%). Similar values of TS and EM were reported by Rhim (2012) for agar/ κ -
361 carrageenan blend films.

362 As glycerol content increased in the formulation (**PG₁** and **PG₂**), films progressively
363 decreased TS and EM ($p < 0.05$), and gradually increased EAB ($p < 0.05$). These results
364 were expected because glycerol acts as a plasticizer on **P** matrix interfering with the
365 formation of polymer-polymer interactions and favored by the additional plasticizing
366 effect of excess water absorbed by glycerol. In this sense, a small increase in glycerol
367 level results in a large drop in tensile strength with concomitant increase of elongation

368 at break (EAB) and WVP (Debeaufort and Voilley 1997; Tanaka et al. 2001; Fairley
369 et al. 1996).

370 As shown in **Figure 1**, **PCa**, **PCaG₁** and **PCaG₂** films exhibited higher EAB and
371 lower TS and EM values than **P**, **PG₁** and **PG₂**, respectively ($p < 0.05$). It seems that
372 Ca^{2+} also exerts a plasticizing effect on **P** matrix with and without glycerol. These
373 results can be related to that Ca^{2+} increases water content of **P** matrix. And in this
374 regard, as was previously mention, water molecules could act as strong plasticizers
375 because their increase molecular mobility and elasticity in the rubbery state
376 (Karbowiat et al. 2006). According to Sothornvit and Krochta (2000) there are two
377 main types of plasticizers: 1. Molecules capable of forming hydrogen bonds, thus
378 interacting with polymers by interrupting polymer-polymer bonding and maintaining
379 the furthers distance between polymers chains, 2. Molecules capable of interact with
380 large amounts of water to retain more water molecules, thus resulting in higher
381 moisture content and larger hydrodynamic radius. In this case, it seems that both, the
382 plasticizing effect of glycerol and Ca^{+2} could be associated to both described
383 mechanisms.

384 *Films microstructure*

385 **Figure 2** shows SEM micrographs of surface and cross-section of films. **P** film was
386 characterized by a compact, uniform, dense structure and homogenous appearance,
387 indicating a good compatibility between carrageenans/porphyrans from *P. columbina*
388 aqueous fraction. **P**, **PG₁** and **PG₂** films micrographs showed slightly rough surfaces
389 without any pores. The roughness becomes less noticeable by increasing the
390 proportion of glycerol in the formulation. As can be seen, Ca^{+2} addition increased the
391 films roughness, being more evident in **PCa**. As glycerol proportion increased in

392 these formulations, rough surfaces also gradually decreased (**PCaG₁** and **PCaG₂**
393 films). These results are in agreement with those reported by Bosquez-Molina et al.
394 (2010) for mesquite gum based edible films containing different concentrations of
395 CaCl₂ (0.0, 0.1, 0.2, 0.3, 0.4 or 0.5 g/100 g) plus glycerol (1.5 g/100 g).
396 SEM micrographs of cross-section films (**Figure 2**) confirm that Ca⁺² addition
397 significantly increased film thickness, being this effect clearly seen in **PCaG₁** film.
398 Therefore, Ca²⁺ would interact with sulfate groups opening film structure, promoting
399 water retention and increasing film thickness, causing a net plasticizer effect on the
400 films network that was reflected in their mechanical properties and water
401 susceptibility.
402 Although Ca⁺² addition did not exert the expected cross-linking effect, improving the
403 mechanical and/or barrier properties of films, their interactions with the sulphate
404 groups was verified by FTIR. Infrared spectroscopy is a rapid and non-destructive
405 technique that has been widely used to characterize different polysaccharides
406 (Martins et al. 2012). **Figure 3** shows FTIR spectrum (1400-700 cm⁻¹) of **P** and **PCa**
407 films. Usually, this region is used to obtain information on the structure of
408 phycocolloids (agars and carrageenans). **P** spectra shows the characteristic bands of
409 agarocolloids like porphyran (1372, 1250, 1150, 1076, 933, 890, 820 and 771 cm⁻¹).
410 These results agree with those reported by Zhang et al. (2005) for *P. capensis*
411 phycocolloids. The bands at 1370 and 1250 cm⁻¹ can be attributed to the S=O
412 vibration of the sulphate groups. The important band at 1076 cm⁻¹ corresponds to the
413 skeleton of galactans, while the band at 890 cm⁻¹ is assigned specifically to agar
414 specific bands. Bands at 930 cm⁻¹ in the spectra correspond to the C-O-C group of
415 3,6-anhydro- α -L-galactose (Souza et al. 2012). Additionally, the bands at 845, 830
416 and 820 cm⁻¹ are used to infer the position of sulphate group in agarocolloids and are

417 assigned to the 4-sulphate, 2-sulphate and 6-sulphate of D-galactose units,
418 respectively (Maciel et al. 2008; Gómez-Ordoñez and Rupérez 2011). The FTIR
419 spectrum of **P** shows a low intensity band at 845 cm^{-1} , attributed to sulphate
420 substitution at the C-4 of galactose. The presence of a small peak at 820 cm^{-1} could
421 indicate a low degree of substitution on C-6. The absence of bands at 830 cm^{-1}
422 indicates that 2-sulphate galactose and sulphate on the C-2 of 3,6-anhydro- α -L-
423 galactose are not present. These results are in agreement with those reported by Melo
424 et al. (2002) and Maciel et al. (2008) who worked with two different red seaweeds.
425 Also, the little band at 890 cm^{-1} could be attributed to anomeric CH of β -
426 galactopyranosyl residues. Finally, the bands at 1150 and 775 cm^{-1} can be assigned to
427 C-O stretching vibrations of pyranose ring, in agreement the FTIR spectrum of
428 different red seaweed reported by Gómez-Ordoñez and Rupérez (2011). On the other
429 hand, only for **PCa** spectrum, lower absorbance at 1372 , 1250 and 820 cm^{-1} than **P**
430 was observed. Therefore, the addition of Ca^{+2} could affect spectroscopic behavior of
431 sulphate groups present in phycocolloids. In this sense, Sartori et al. (1997) found that
432 the addition of CaCl_2 to alginate films produced a large shift at 1420 cm^{-1} (COO-
433 symmetrical stretch peak), reducing band intensity. In that work, the absorbance
434 reduction was associated to the replacement of sodium by calcium, which changes
435 charge density, the radius and the atomic weight of the cation associate to the
436 hydrocolloid, creating a new environment around the carbonyl groups (Sartori et al.
437 1997). This phenomenon could also occur in **PCa** films where calcium would replace
438 sodium associated with sulfate group. Furthermore, rates of absorbance at $1250\text{ cm}^{-1}/$
439 2920 cm^{-1} and $1370\text{ cm}^{-1}/2920\text{ cm}^{-1}$ are indexes which relate total sulfate to sugar
440 content (Melo et al. 2002; Rochas et al. 1986). These ratios were 1.5 and 0.9 for **P**
441 films; and 1.1 and 0.6 for **PCa** films. These results are in concordance with those

442 mentioned before and suggest a possible effect of Ca^{+2} on sulphate group from agars
443 and/or carrageenans.

444

445 **Conclusions**

446 It was possible to produce biodegradable films based on phycocolloids
447 (carrageenans/porphyrans) extracted from *Pyropia columbina* with a wide range of
448 mechanical properties by incorporation of glycerol and/or Ca^{+2} into film-forming
449 dispersions. The addition of glycerol to film-forming dispersions without Ca^{2+} allowed
450 producing less resistant but more stretchable and water susceptible films (with higher
451 water solubility and water vapor permeability) than those produced in the absence of
452 plasticizer. Regarding calcium addition, in some properties Ca^{2+} masks glycerol effect
453 (water solubility and water vapor permeability), but in others, the effect of calcium is
454 added to plasticizer glycerol effect (mechanical properties). Calcium could stabilize the
455 three-dimensional structure of **P** phycocolloids by interactions between sulfate groups,
456 promote water retention and open film structure.

457

458 **Acknowledgements**

459 The authors are thankful to the National Agency of Scientific and Technological
460 Support (SECyT, PICT-2010-1837), the Universidad Nacional de La Plata (11-X494)
461 and the Universidad Nacional del Litoral (CAI+D 2011 PI 0292 LI) for their financial
462 support.

463

464 **Conflicts of interest**

465 The authors declare no conflicts of interest

467 **References**

- 468 Al-Alawi A, Al-Marhubi I, Al-Belushi M, Soussi B (2011) Characterization of
469 Carrageenan extracted from *Hypnea bryoides* in Oman. *Marine Biotechnol* 13:893–899.
- 470 ASTM (2004) Annual book of ASTM standards; ASTM International: Philadelphia,
471 PA, USA.
- 472 Baldwin E, Hagenmaier R, Bai J (2012) Edible coatings and films to improve food
473 quality (second edition). CRC Press, Boca Raton, USA.
- 474 Blanco Pascual N, Gómez-Guillén C, Montero P (2014) Integral *Mastocarpus stellatus*
475 use for antioxidant edible film development. *Food Hydrocolloids* 40:128-137.
- 476 Bosquez-Molina E, Tomás S, Rodríguez-Huezo M (2010) Influence of CaCl₂ on the
477 water vapor permeability and the surface morphology of mesquite gum based edible
478 films. *Food Sci Technol* 43:1419-1425.
- 479 Cian R, Salgado P, Drago S, González R, Mauri A (2014) Development of naturally
480 activated edible films with antioxidant properties prepared from red seaweed *Porphyra*
481 *columbina* biopolymers. *Food Chem* 146:6-14.
- 482 Debeaufort F, Voilley A (1997) Methylcellulose-based edible films and coatings: 2.
483 Mechanical and thermal properties as a function of plasticizer content. *J. Agric. Food*
484 *Chem* 45:685–689.
- 485 Fabra M, Talens P, Chiralt A (2010) Influence of calcium on tensile, optical and water
486 vapour permeability properties of sodium caseinate edible films. *J Food Eng* 96:356–
487 364.
- 488 Fairley P, Monahan F, German J, Krochta J (1996) Mechanical properties and water
489 vapor permeability of edible films from whey protein isolate and sodium dodecyl
490 sulfate. *J Agric Food Chem* 44:438-443.

491 Fang Y, Tung M, Britt I, Yada S, Dalgleish D (2002) Tensile and Barrier Properties of
492 Edible Films Made from Whey Proteins. *Food Eng Phys Prop* 67:188-193.

493 García M, Pinotti A, Zaritzky N (2006) Physicochemical, Water Vapor Barrier and
494 Mechanical Properties of Corn Starch and Chitosan Composite Films. *Starch/Stärke*
495 58:453–463.

496 Ghorpade V, Li H, Gennadios A, Hanna M (1995) Chemically modified soy protein
497 films. *Transactions ASAE* 38:1805 – 1808.

498 Giménez B, López de Lacey A, Pérez-Santín E, López-Caballero M, Montero P (2013)
499 Release of active compounds from agar and agar-gelatin films with green tea extract.
500 *Food Hydrocolloids* 30:264 – 271.

501 Gómez-Ordóñez E, Rupérez P (2011) FTIR-ATR spectroscopy as a tool for
502 polysaccharide identification in edible brown and red seaweeds. *Food Hydrocolloids* 25:
503 1514 – 1520.

504 Gontard N, Duchez C, Cuq J, Guilbert S (1994) Edible composite films of wheat gluten
505 and lipids: water vapour permeability and other physical properties. *Int. J. Food Sci.*
506 *Technol* 29: 39 – 50.

507 Gontard N, Guilbert S, Cuq J (1993) Water and glycerol as plasticizers affect
508 mechanical and water vapor barrier properties of an edible wheat gluten film. *J. Food*
509 *Sci* 58:206-211.

510 Han J, Gennadios A (2005) Edible films and coatings: a review. In J. H. Han (Ed.),
511 *Innovations in food packaging* (pp. 239-262). San Diego, CA: Elsevier Academic Press

512 Hernández-Muñoz P, Villalobos R, Chiralt A (2004) Effect of thermal treatments on
513 functional properties of edible films made from wheat gluten fractions. *Food*
514 *Hydrocolloids* 4:647 – 654.

515 Janaswamy S, Chandrasekaran R (2002) Effect of calcium ions on the organization of
516 iota-carrageenan helices: an X-ray investigation. *Carbohydrate Res* 337:523–535.

517 Karbowski T, Debeaufort F, Champion D, Voilley A (2006) Wetting properties at the
518 surface of iota-carrageenan-based edible films. *J Colloid Interface Sci* 294:400–410.

519 Krikor H, Tarrago S, Jansen C (2011) Polymeric Material for Making a Packaging
520 Article Having Oxygen-Barrier Properties and Low Light. United States Patent
521 Application 20110244155.

522 Leiria Campo V, Kawano D, da Silva Jr D, Carvalho I (2009) Carrageenans: Biological
523 properties, chemical modifications and structural analysis– A review. *Carbohydrate*
524 *Polym* 77:167–180.

525 Lizarraga M, De Piante Vicin D, González R, Rubiolo A, Santiago L (2006)
526 Rheological behaviour of whey protein concentrate and λ -carrageenan aqueous
527 mixtures. *Food Hydrocolloids* 20:740-748.

528 Maciel J, Chaves L, Souza B, Teixeira D, Freitas A, Feitosa J, de Paula R (2008)
529 Structural characterization of cold extracted fraction of soluble sulfated polysaccharide
530 from red seaweed *Gracilaria birdiae*. *Carbohydrate Polym* 71:559 – 565.

531 Marcotte M, Taherian Hoshahili A, Ramaswamy H (2001) Rheological properties of
532 selected hydrocolloids as a function of concentration and temperature. *Food Res Int* 34:
533 695-703.

534 Martins J, Cerqueira M, Vicente A (2012) Influence of α -tocopherol on
535 physicochemical properties of chitosan-based films. *Food Hydrocolloids* 27:220-227.

536 Melo M, Feitosa J, Freitas A, de Paula R (2002) Isolation and characterization of
537 soluble sulfated polysaccharide from the red seaweed *Gracilaria cornea*. *Carbohydrate*
538 *Polym* 49:491 – 498.

539 Olivasa G, Barbosa-Cánovas G (2008) Alginate–calcium films: Water vapor
540 permeability and mechanical properties as affected by plasticizer and relative humidity.
541 LWT- Food Sci Technol 41:359–366.

542 Rhim J (2004) Physical and mechanical properties of water resistant sodium alginate
543 films. LWT- Food Sci Technol 37:323–330.

544 Rhim J (2012) Physical-mechanical properties of agar/κ-carrageenan blend film and
545 derived clay nanocomposite film. J Food Sci 77:66–73.

546 Rochas C, Lahaye M, Yaphe W (1986) Sulfate content of carrageenan and agar
547 determined by infrared spectroscopy. Botanica Marina 29:335-340.

548 Salgado P, Molina Ortiz S, Petruccelli S, Mauri A (2010) Biodegradable sunflower
549 protein films naturally activated with antioxidant compounds. Food Hydrocolloids,
550 24:525-533.

551 Sartori C, Finch D, Ralph B (1997) Determination of the cation content of alginate thin
552 films by FTIR spectroscopy. Polymer 38:43-51.

553 Shaw N, Monahan F, O’riordan E, O’sullivan M (2002) Physical Properties of WPI
554 Films Plasticized with Glycerol, Xylitol, or Sorbitol. Food Eng Phys Prop 67:164-167.

555 Sothornvit R, Krochta J (2000) Plasticizer effect on oxygen permeability of beta-
556 lactoglobulin films. J. Agric. Food Chem 48:6298-6302.

557 Sousa A, Sereno A, Hilliou L, Goncalves M (2010) Biodegradable agar extracted from
558 *Gracilaria Vermiculophylla*: film properties and application to edible coatings.
559 Materials Science Forum Vols 636-637:739-744.

560 Souza B, Cerqueira M, Bourbon A, Pinheiro A, Martins J, Texeira J, Coimbra M,
561 Vicente A (2012) Chemical characterization and antioxidant activity of sulfated
562 polysaccharide from the red seaweed *Gracilaria biridiae*. Food Hydrocolloids 27:287–
563 292.

564 Tanaka M, Iwata K, Sanguandeeikul R, Handa A, Ishizaki S (2001) Influence of
565 plasticizers on the properties of edible films prepared from fish water-soluble proteins.
566 *Fisheries Sci* 67:346–351.

567 Thrimawithana T, Young S, Dunstan D, Alany (2010) Texture and rheological
568 characterization of kappa and iota carrageenan in the presence of counter ions.
569 *Carbohydrate Polym* 82:69-77.

570 Vieira M, da Silva M, dos Santos L, Beppu M (2011) Natural-based plasticizers and
571 biopolymer films: A review. *Eur Polym J* 47:254-263.

572 Wolfenden J, Robinson D, Cape J, Paterson I, Francis B, Mehlhorn H, Wellburn A
573 (1988) Use of carotenoid ratios, ethylene emissions and buffer capacities for the early
574 diagnosis of forest decline. *New Phytol* 109:85-95.

575 Zhang Q, Qi H, Zhao T, Deslandes E, Ismaeli N, Molloyd F, Critchley A (2005)
576 Chemical characteristics of a polysaccharide from *Pyropia capensis* (Rhodophyta).
577 *Carbohydrate Res* 340:2447–2450.

578

Figure Captions

579

580 **Fig. 1** Mechanical properties measured in tensile tests: **A)** Tensile strength (TS), **B)**
581 Elongation at break (EAB), and **C)** Elastic modulus (EM) of films obtained from
582 phycocolloids-enriched fractions (**P**) from *P. columbina* added with glycerol and/or
583 calcium. G₁: 12.5 g glycerol/100 g dry solid; G₂: 25 g glycerol/100 g dry solid and Ca:
584 16 g Ca⁺²/100 g dry solid. Results are expressed as mean value ± standard deviation.
585 Different letters in the bars mean significant differences between samples (p < 0.05),
586 according to Fisher's least significant difference test.

587

588 **Fig. 2** Scanning electron microscopy (SEM) of films obtained from phycocolloids-
589 enriched fractions (**P**) from *P. columbina* added with glycerol and/or calcium. G₁: 12.5
590 g glycerol/100 g dry solid; G₂: 25 g glycerol/100 g dry solid and Ca: 16 g Ca⁺²/100 g
591 dry solid. SEM images magnifications: 50X for films surface and 100X for films cross-
592 section.

593

594 **Fig. 3** FTIR spectrum (1400 to 700 cm⁻¹) of films obtained from phycocolloids-enriched
595 fractions (**P**) and phycocolloids-enriched fractions added with calcium at 16 g Ca⁺²/100
596 g dry solid (**PCa**).

597

Fig. 1

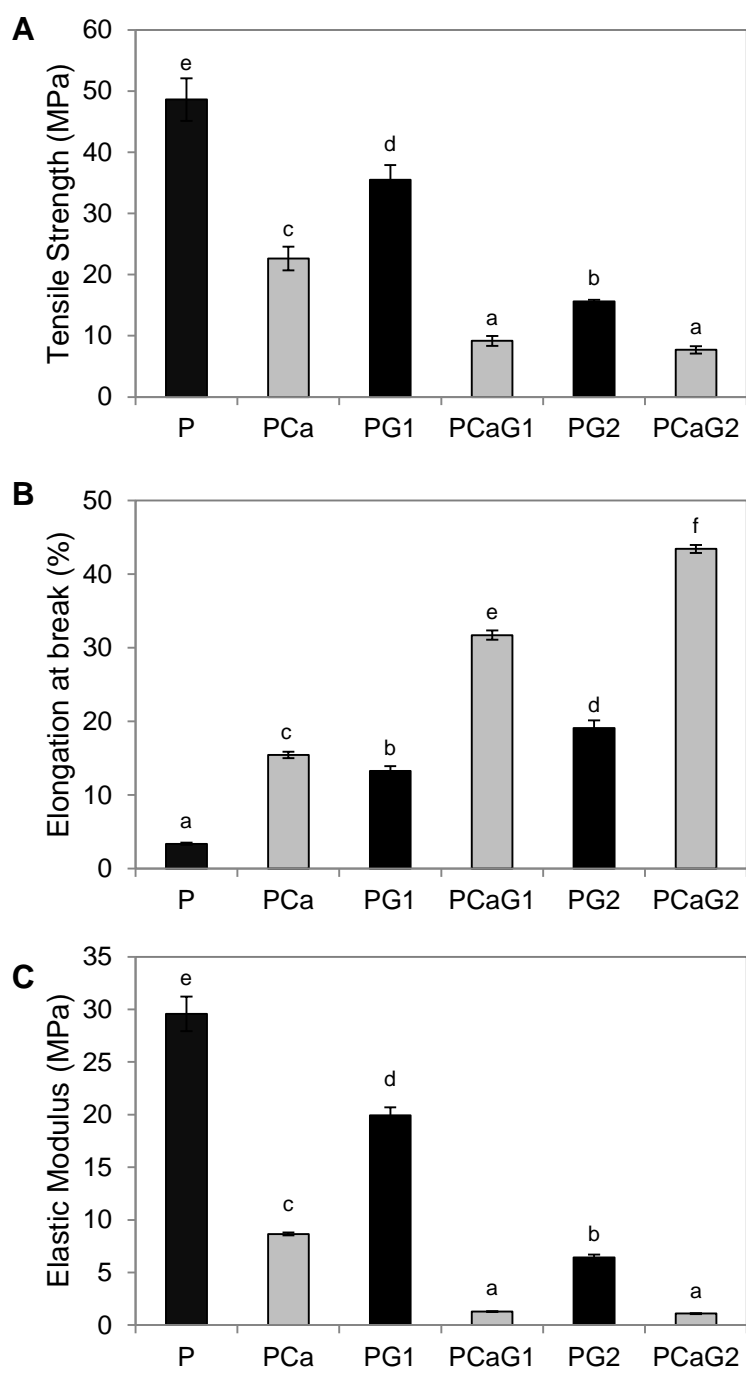


Fig. 2

Films obtained from phycocolloids-enriched fractions (**P**) from *P. columbina*

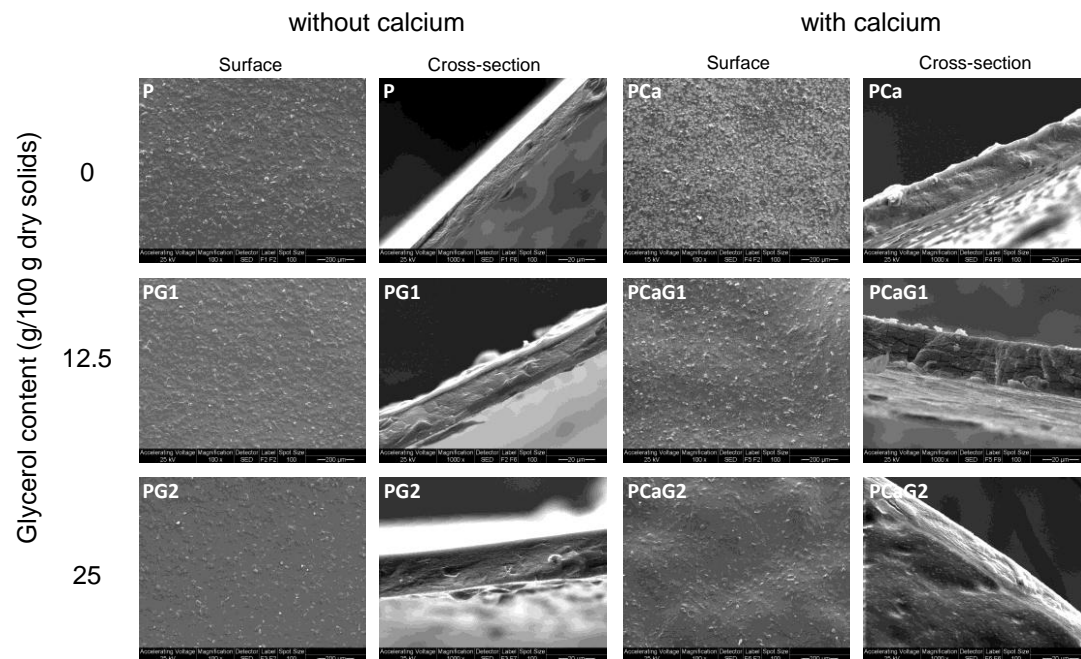
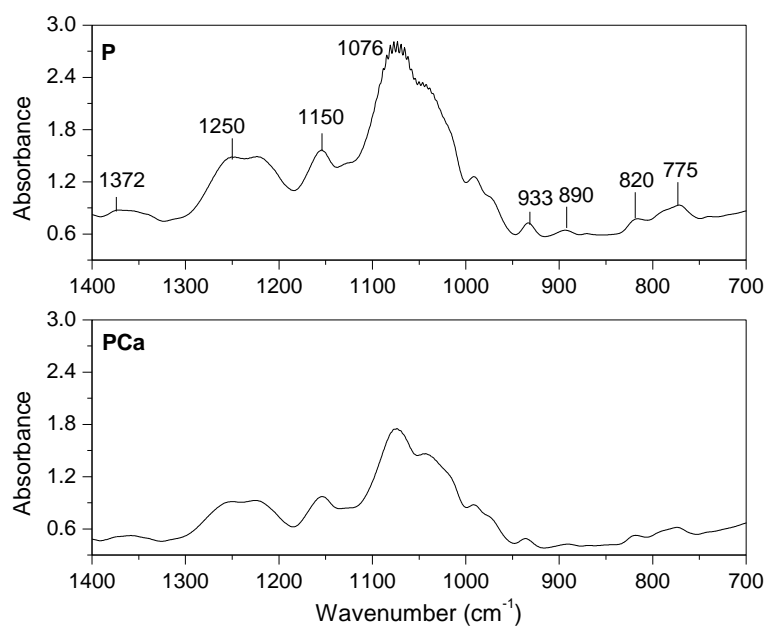


Fig. 3



- 1 **Table 1.** Rheological behavior of film-forming dispersions obtained from phycocolloids-enriched fractions (**P**) added with glycerol and/or
 2 calcium.

Formulations	Ostwald de Waele parameters		Apparent viscosity (mPa s)		
	K (Pa s ⁿ)	n	D=60 s ⁻¹	D=300 s ⁻¹	D=500 s ⁻¹
P	2.15 ± 0.28 ^b	0.47 ± 0.01 ^a	233 ± 28 ^b	104 ± 12 ^{ab}	78 ± 9 ^a
PG₁	2.16 ± 0.03 ^b	0.47 ± 0.01 ^a	233 ± 1 ^b	107 ± 2 ^b	79 ± 2 ^a
PG₂	2.05 ± 0.13 ^b	0.47 ± 0.01 ^a	235 ± 16 ^b	104 ± 7 ^{ab}	79 ± 8 ^a
PCa	1.59 ± 0.05 ^a	0.50 ± 0.01 ^b	205 ± 5 ^a	96 ± 1 ^{ab}	72 ± 1 ^a
PCaG₁	1.57 ± 0.04 ^a	0.50 ± 0.01 ^b	199 ± 1 ^a	93 ± 1 ^{ab}	69 ± 1 ^a
PCaG₂	1.50 ± 0.06 ^a	0.51 ± 0.01 ^b	195 ± 8 ^a	91 ± 3 ^a	69 ± 2 ^a

3

- 4 G₁: 12.5 g glycerol/100 g dry solid; G₂: 25 g glycerol/100 g dry solid and Ca: 16 g Ca⁺²/100 g dry solid. Results are expressed as mean value ± standard deviation. Different
 5 letters in the same column mean significant differences between samples (p < 0.05), according to Fisher's least significant difference test.

1 **Table 2.** Thickness, CIE-Lab color parameters (L^* , a^* and b^*), total color difference (ΔE^*), chroma (C^*), hue (h) and opacity of films obtained
 2 from phycocolloids-enriched fractions (**P**) with glycerol and/or calcium.

3

Formulations	Thickness (μm)	Color parameters						Opacity x 10^{-4} (UA)
		L^*	a^*	b^*	ΔE^*	C^*	h	
P	16.1 ± 0.2^a	$79,4 \pm 1,0^b$	$-3,1 \pm 0,1^b$	$20,6 \pm 0,5^b$	26.3 ± 0.5^a	20.9 ± 0.7^a	98.6 ± 0.3^a	14.3 ± 0.0^b
PG1	17.1 ± 0.2^a	$80,0 \pm 0,6^b$	$-3,2 \pm 0,2^b$	$20,6 \pm 0,9^b$	25.9 ± 0.4^a	20.8 ± 1.3^a	98.8 ± 0.6^a	11.7 ± 0.1^a
PG2	18.0 ± 2.3^a	$79,6 \pm 0,8^b$	$-3,2 \pm 0,1^b$	$20,5 \pm 0,3^b$	26.1 ± 0.5^a	20.7 ± 0.3^a	98.7 ± 0.2^a	10.4 ± 1.2^a
PCa	21.3 ± 0.9^b	$77,9 \pm 0,6^a$	$-2,9 \pm 0,0^a$	$19,5 \pm 0,3^a$	26.5 ± 0.4^a	19.7 ± 0.4^a	98.4 ± 0.3^a	14.1 ± 0.2^b
PCaG1	21.6 ± 0.4^b	$77,9 \pm 1,1^a$	$-2,9 \pm 0,0^a$	$19,5 \pm 0,5^a$	26.5 ± 0.7^a	19.7 ± 0.7^a	98.5 ± 0.3^a	10.5 ± 0.4^a
PCaG2	21.9 ± 0.7^b	$77,6 \pm 1,0^a$	$-2,9 \pm 0,0^a$	$19,3 \pm 0,2^a$	26.7 ± 0.8^a	19.6 ± 0.3^a	98.6 ± 0.2^a	10.4 ± 1.7^a

4

5 G_1 : 12.5 g glycerol/100 g dry solid; G_2 : 25 g glycerol/100 g dry solid and Ca: 16 g Ca^{+2} /100 g dry solid. Results are expressed as mean value \pm standard deviation. Different
 6 letters in the same column mean significant differences between samples ($p < 0.05$), according to Fisher's least significant difference test.

1 **Table 3.** Moisture content (MC), water solubility (WS) and water vapor permeability (WVP) of films obtained from phycocolloids-enriched
 2 fractions (**P**) from *P. columbina* added with glycerol and/or calcium.

3

Formulations	MC	WS	WVPx10¹¹
	(g 100 g ⁻¹)	(%)	(g H ₂ O Pa ⁻¹ s ⁻¹ m ⁻¹)
P	10.7 ± 0.2 ^a	84.5 ± 2.2 ^a	4.9 ± 0.1 ^a
PG₁	11.9 ± 0.4 ^b	95.0 ± 0.2 ^b	5.2 ± 0.1 ^b
PG₂	16.0 ± 0.4 ^c	95.1 ± 2.2 ^b	5.2 ± 0.2 ^b
PCa	17.0 ± 0.6 ^d	96.3 ± 1.6 ^{bc}	6.7 ± 0.1 ^c
PCaG₁	18.7 ± 0.4 ^e	98.1 ± 0.8 ^c	6.8 ± 0.1 ^c
PCaG₂	18.9 ± 0.3 ^e	98.7 ± 0.7 ^c	6.6 ± 0.2 ^c

4

5 G₁: 12.5 g glycerol/100 g dry solid; G₂: 25 g glycerol/100 g dry solid and Ca: 16 g Ca⁺²/100 g dry solid. Results are expressed as mean value ± standard deviation. Different
 6 letters in the same column mean significant differences between samples (p < 0.05), according to Fisher's least significant difference test.

7

8